

# Informing Observatory Operations with Accessible Telemetry and Performance Metrics

Daniel R. Harbeck <sup>a</sup>, Annie Kirby<sup>a</sup>, Lindy Lindstrom<sup>a</sup>, Nikolaus Volgenau<sup>a</sup>, and Mark Bowman <sup>a</sup>

<sup>a</sup>Las Cumbres Observatory, Goleta, CA 93117 USA

## ABSTRACT

The operation of robotic telescopes at remote locations without supervision by local staff is a specific challenge for Las Cumbres Observatory's (LCOGT) global network, where more than 25 telescopes are operated at seven globally distributed sites. LCOGT personnel typically visits each site every 18 months for general maintenance and upgrade tasks, whereas minor failures are handled by local site support staff.

LCOGT is making efforts to quantitatively inform decisions about scheduling preventative maintenance tasks and to provide tools to assist with failure diagnostic and response. For example, all night-time observations from all telescopes are analyzed to quantify the telescopes' throughput; these data, updated daily and looking back more than four years, are used to inform the cadence of telescope mirror washing and recoating. Further examples of utilizing every day's science data are presented, including monitoring the readnoise of more than 25 CCD cameras which has enabled the early detection of a failing CCD controller. Telemetry from all installations is collected in a no-SQL database ([OpenSearch](#))<sup>\*</sup> and presented to various stakeholders via the visualization tools [Kibana](#) and [Grafana](#)<sup>†</sup>. These utilities are used to diagnose problems in preprogrammed views, e.g., to detect acute issues or long-term degradation in the fleet of Cryotiger cooling systems.

Telemetry data and performance metrics have always been collected at LCOGT. Making those data consistent, accessible, and easy to use for all stakeholders at LCOGT made the deluge of information usable in the daily observatory operation routine.

**Keywords:** Observatory operations, commissioning, quality control

## 1. INTRODUCTION

Las Cumbres Observatory (LCOGT) operates a network of more than 25 robotic telescopes at seven sites around the globe<sup>1</sup> to enable time domain observation capability in astronomy. The current fleet of telescopes consists of two 2-meter class telescopes, thirteen 1-meter class telescopes, and ten 40 cm class telescopes. The sites, enclosures, telescopes, and instruments operate autonomously under software control. Observation requests are dispatched by a central scheduler program and then executed on-site; the schedule is recomputed about every five to ten minutes.<sup>2</sup> Staff are not directly involved in the operation of the telescopes, although high-level supervision is provided by a globally distributed team of about four staff members, who identify and attempt to resolve system failures, or escalate them to domain experts if not immediately resolvable.<sup>3</sup>

At a given time there are one or maybe two staff members actively monitoring the network. As there are more than 25 telescopes and their multiple instruments to be supervised, this monitoring task cannot be approached by observing each individual telescope, and automatic exception detection and alerting plays a key role in keeping the observatory scientifically productive.

Obvious malfunctions of an instrument or telescope (e.g., a cooling failure of a CCD camera or a telescope axis stuck in a hard stop position) can be detected by the site software, as those create well-described and propagated error conditions. Some more subtle issues can also be addressed in the data processing stage: Data products from the observatories are automatically uploaded into a central archive that is hosted in the Amazon cloud (Amazon Web Services, AWS), and processed there with automated data pipelines (e.g., BANZAI for all

---

<sup>\*</sup><https://www.elastic.co/>, <https://opensearch.org/>

<sup>†</sup><https://grafana.com/oss/>

CCD imaging cameras<sup>4,5</sup>). The BANZAI pipeline has built-in quality control measures to detect and report gross deviations of data products from their expectation, such as a large change in a flat field image from a reference image or the detection of saturation of most pixels. But without a person overlooking all images and being intimately familiar with each telescope, as would be the case in visitor or service mode observing, subtle changes in the telescope and instrument performance are not easily detected and can remain unnoticed, possibly growing into larger issues.

To further support various stakeholders in operations (engineering, science operations) to effectively operate the telescope network, we identified the need to present observatory state information in an easy and user-friendly way. In this paper, we present several case studies how we use telemetry and performance parameters derived from science data as a tool to assess the general health, while simultaneously detecting systematic error sources and degradation trends in our system of robotic telescopes.

Monitoring the evolution of performance metrics over time is one canonical tool available at every observatory. At LCOGT with several identical-design installations worldwide, we can also compare differential changes between telescope and instrument instances.

## 2. PRESENTING TELEMETRY DATA & ISSUING AUTOMATIC ALERTS

The LCOGT system was intended to be robotically operated, hence remote control and storing of telemetry and log files are part of the software design. Status data originating from the telescopes is collected independently from the scientific data, and is transferred directly into an [OpenSearch](#) database hosted in AWS. The data is made accessible to staff via the [OpenSearch](#) API and online visualization tools such as [Grafana](#) and [OpenSearch](#) dashboards. The [OpenSearch](#) dashboards interface is used predominantly for exploratory work on data.

Data visualization tools such as [Grafana](#) have been established by the software and IT groups to monitor the state of various software deployments. Upon first experiments in 2018 by the science support and engineering groups, the ease of creating reusable graphical representations of telemetry led to a wide acceptance beyond the software group. Now, four years later, it became an indispensable tool for repetitive performance monitoring and error diagnostics.

Monitoring a data dashboard still requires a significant commitment of time and resources, and to further automate observatory monitoring, we started using [Grafana](#)'s alarming function to automatically detect fault conditions and propagate those to relevant personnel. Most real-time communication at LCOGT is handled via the Slack application and we utilize the tight integration of [Grafana](#) and Slack to send out alarms into the appropriate Slack channels.

In the following, we will discuss some of the monitoring and alerting use cases we developed around the telemetry data and [Grafana](#) and also how we distribute actionable alerts to avoid alarm fatigue.

### 2.1 Monitoring the health of the Cryotiger-cooled cameras

The primary cameras on the 1-meter network are made of Fairchild CCD486 detectors in a custom-designed cryostat to cool the detectors to -90 degrees C; the design is called Sinistro. In total, LCO operates 16 such cameras in the network (12 as primary imagers, and 4 as science cameras in the NRES spectrograph network). As daily filling of liquid nitrogen tanks is not compatible with our robotic observation paradigm, the cooling is achieved via closed cycled coolers (Polycold / Brooks / Edwards Cryotiger). The cryosystem of the Sinistro cameras is a main weak spot in the operation of the LCOGT network, and whenever a camera warms up the root cause needs to be identified so the appropriate corrective action can be taken. We created [Grafana](#) dashboards that show timeline plots of key operational metrics of each camera on a single page, including: Cryotiger supply and return pressure, detector and cold head temperature, temperature regulator power, pressure in the cryostat, and ambient temperature. With all these data quickly accessible on one page, and the history of data available in user-selected time ranges, it is easier to diagnose an actual issue and distinguish between, e.g., a soft vacuum and a blockage in the cold head. The timeline representation of the operational parameters helps to provide insight on how the cameras react to an intervention, and whether further action is required.

The long-term graphing of the operational parameters over the course of months can help to identify issues early. For example, one Cryotiger installation developed a very slow leak at a telescope at Teide Observatory.

The leak manifested as a reduction in the Cryotiger gas supply pressure over time. As the ambient temperature during that time also declined (local fall to winter transition), we compared the supply pressure to a similar installation at the same site and concluded that the pressure decline was disproportionately higher at the system in question, and hence was not simply related to a falling temperature but a real problem (see Fig. 1). As a consequence, we scheduled leak checking and recharging of the system. No leak was identified at that time, but the Cryotiger compressor was exchanged as a precautionary measure. After continued monitoring, it became clear that the gas leak was not caused by the compressor and remains still present, and is subject to further action.



Figure 1. Pressure of the Cryotiger cooling system (green line) monitored for the two Sinistro cameras at the Teide site. The system in dome A has lost considerable pressure over the course of a year. A leak was speculated in the compressor, however, after a recharge and compressor exchange in May 2022 the pressure continued to decline.

## 2.2 Identifying the state of consumables in the NRES spectrograph system

At four sites we operate nodes of the Network of Robotic Echelle Spectrographs (NRES). Each node is a fiber-fed high-resolution, temperature- and pressure-stabilized spectrograph designed for the measurement of radial velocities of stars to detect orbiting exoplanets. The pressure in the spectrographs is controlled to be slightly above ambient pressure, and the regulator is fed high-purity dry air from a gas bottle. Every couple of months, the dry air tanks require replacement. At the start of NRES operations, the remaining pressure (which is electronically measured and logged in our telemetry database) was regularly checked for each site by a LCOGT staff member on a **Grafana** plot (Fig. 2). As this manual polling became tedious – how often do you need to check: every week? every month? – we introduced **Grafana** alerting on a low-pressure threshold of 200 psi. In our experience that would allow for a remaining operating time of about two weeks and allows for some flexibility for site staff to fold our request into preplanned activities. **Grafana** will now send out a message into a Slack channel related to regular maintenance (in Fig. 2 red dotted lines), and an engineer would then contact site support to schedule the dry air bottle exchange. The automated monitoring of a consumable has freed up staff from a repetitive monitoring task that is now event-driven. There is still a need to monitor the relevant notification in slack channels, but now other interrupt requests are bundled and make the supervising tasks easier.

## 2.3 Telescope focus relevant data

In 2019-2020, we undertook a thorough investigation of the focus stability of the network's 1-meter telescopes. The investigation resulted in the implementation of various changes to improve the telescopes' focus,<sup>3</sup> including (i) improving the function fit to focus curve data, (ii) adjusting the timing of focus corrections to accommodate the rapidly changing thermal environment around the telescopes at the start-of-night, and (iii) employing the off-axis guide cameras as focus sensors for the science cameras. To assess the effects of these various improvements, as well as to monitor the focus performance of the telescopes in general, we created a suite of monitoring tools in **Grafana**. Perhaps the most useful of these is a dashboard for "Focus Relevant Data", which superimposes the values for the median FWHM of extracted sources from each science image on the FWHM of DIMM (Difference Image Motion Monitor) seeing data for the sites which have DIMMs. (See Fig. 3.) The superposition of data

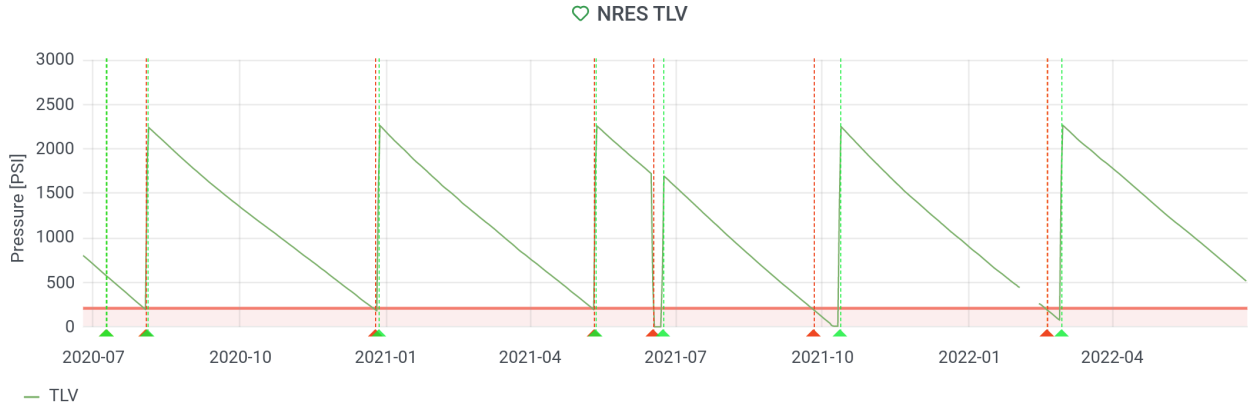


Figure 2. Example of monitoring the dry air supply pressure at the NRES installation at the Wise observatory. When the pressure falls below the threshold of 200psi, a message is sent out to LCOGT staff to request a dry air bottle exchange.

allows operations personnel to quickly determine whether the trend in image FWHM deviate from the site seeing. Additional data displayed in the dashboard show whether environmental changes (such as the ambient temperature, airmass, and wind speed) correlate with changes in the image FWHM.

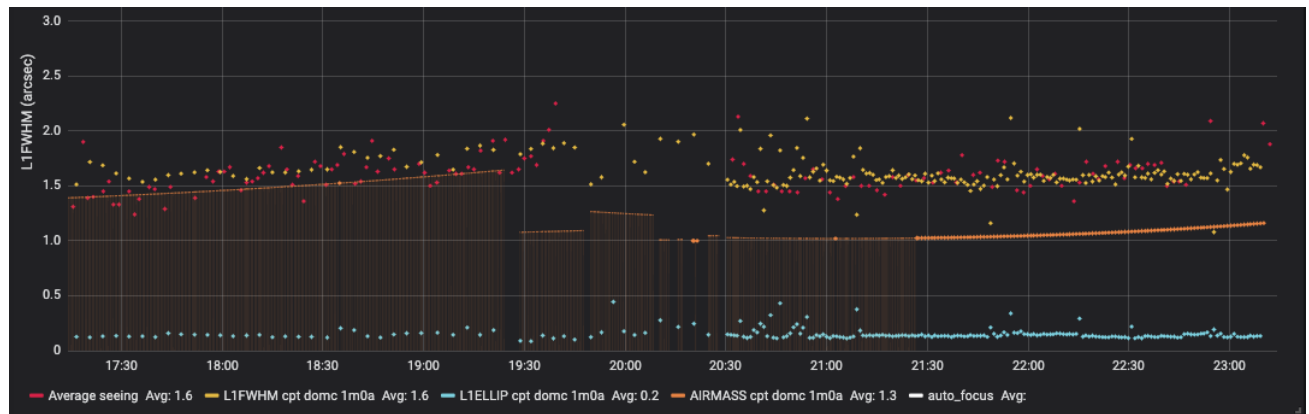


Figure 3. A panel from the Focus Relevant Data Grafana dashboard, showing data from the 1-meter telescope in Dome C at the SAAO (CPT). Over the time interval displayed, the FWHM of sources extracted from science images (yellow dots) are approximately the same as the atmospheric seeing (red dots).

An “Alert:AutoFocus Failures” dashboard displays a timeline of when focus checks fail, as well as tabular information (culled from the logs) to identify the specific telescopes, times, and reasons why the failures occurred. Failures that occur at the start of a telescope’s night (i.e. at the most critical time) automatically trigger an alert, which is sent to an `#alerts-actionable` Slack channel. All network monitors subscribe to that channel, and the alert notifies them to inspect a telescope’s focus before the night’s science observations commence. (Even if the check fails, the focus may be fine.) The average alert rate is approximately two in 24 hours. However, focus check failures often cluster (i.e. the checks on several telescopes at one site fail) because of environmental conditions like partly cloudy skies.

The “AutoFocus Failures” dashboard is designed to measure the long-term performance of the focus checks. The panels in the dashboard tally the number of checks that fail at each site over a particular time interval. If one site or telescope shows conspicuously more failures than another, a deeper investigation is undertaken. The dashboard also displays two lists of the reasons for the failures. One list is chronological (most recent failure first); the other list is by error frequency (most common error first).

## 2.4 The targeted audience and avoiding alarm fatigue

In a network of more than 25 telescopes, there will always be some component in an exception state, and it is critical to limit how many alarms are issued, as well as to issue those alarms only to a targeted audience for whom those alarms are meaningful and/or actionable. We follow a few guidelines when integrating alarms into Slack:

1. We separated human-to-human communication from the machine-to-human alarming in separate channels in Slack. As Slack is predominantly used as a human-to-human communication platform, we found it distracting when new out-of-context alert messages would interrupt other ongoing conversations. E.g., at first actionable alarms from telescopes were routed to the communication channel used by the telescope operations team, but we quickly found that the dynamic of alarms and follow-up discussions would not work well in one single channel. We subsequently created dedicated channels for alarm messages.
2. We route alarms into audience-relevant channels: Initially, we routed all alarm messages into a single alarm channel, but this generated too many messages that were irrelevant to most of the individuals who subscribed to that channel, diminishing the usefulness of the alert stream. This was mitigated by routing alarm messages to distinct channels that are relevant for a distinct group: E.g., alerts requiring immediate action, such as the report of an out-of-focus telescope vs. alerts that notify the engineering group about upcoming maintenance needs.
3. Message only when entering a fault state: **Grafana** can send alarms both when entering or clearing a fault condition, as well as when there are no data available (e.g., due to connectivity issues with an observatory). For many alert types, we found it most practical to send alert messages only when entering a fault state to limit the amount of activity in alerting channels.
4. Once defined in **Grafana**, alerts themselves and their thresholds are not set in stone. Some thresholds vary with season (e.g., the Cryotiger supply pressure varies with ambient temperature) and need adjustments <sup>†</sup>, or the initial alert thresholds were adjusted to less aggressive levels. It could also be the case that a fault mode for which an alert was defined turned out to be operationally not as relevant and could be discontinued.

## 3. PERFORMANCE METRICS DERIVED FROM ON-SKY OBSERVATIONS

Telemetry of individual components of a telescope are relevant to diagnosing fault states but do not provide direct insight into the scientific quality of data an observatory produces. We present examples of how we use calibration and science data from all LCOGT telescopes to monitor the health of the telescope and instrumentation as a system. In particular, we will discuss (i) the monitoring of the throughput of all LCOGT's telescopes, (ii) the readnoise performance of the fleet of Archon CCD controllers, and (iii) the seasonal drift in the fiber location in the NRES acquisition and guide unit (AGU). The common theme of all those applications is that we are analyzing data that are collected as part of the regular observing routine and make those results available in a central database for further evaluation.

The data analysis done in those applications resembles typical commissioning (or recommissioning) tasks, where a dedicated instrument or telescope scientist would carefully analyze data taken under controlled conditions. *In our applications we replace the careful analysis and controlled conditions by forcing measurements on data taken every day. The confidence of each individually derived quantity will be diminished, but because we measure performance metrics daily we will get an excellent picture of performance changes in time and between instruments and telescopes.*

The examples below follow the same software design pattern: The LCOGT archive is queried daily for new observations from all relevant telescopes. The selected observations (daytime bias, sky flats, nighttime images, or target acquisition images) are downloaded via an API call from the LCOGT archive and analyzed in a use-case-specific way. The result is stored in a database. A subsequent analysis program fetches records from that

---

<sup>†</sup>as of this writing, **Grafana** does not support alerting on calculated quantities, such as a temperature-corrected pressure

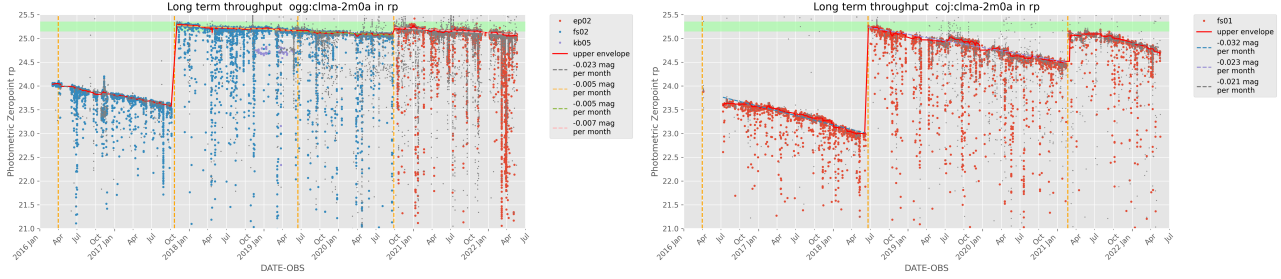


Figure 4. Comparison of the throughput of the LCOGT 2-meter telescopes, located at Haleakalā (Hawaii, left graph) and Siding Springs (Australia, right graph). The mirror at Siding Springs deteriorates much faster than the mirror at the Haleakalā site, which is mostly attributed to the harsher environment there.

database, filtered by camera or telescope, and generates relevant diagnostic plots in a single, comprehensive web page. The database can be queried separately if needed.

All applications are deployed in the Amazon cloud (AWS) and are co-located in the same Amazon region as our archived data, avoiding costs for data transfer in and out of the cloud. For the database backend, we choose Amazon’s Postgres instances, and graphical results (PNG images) are stored in Amazon S3 object stores for later use in a web application. Compute resources are provided via Amazon EC2 instances that are choreographed via Kubernetes.

### 3.1 photzp: Monitoring the throughput of 25 telescopes

The light-collecting power of a reflective telescope is predominantly driven by the primary mirror’s aperture. However, the quality and cleanliness of the reflective coating on a telescope’s mirrors are critically important to utilize the collecting aperture effectively, and keeping a telescope’s optical system clean and free of dust is a typical and labor-intensive routine behind-the-scenes effort at each observatory, involving CO<sub>2</sub>-snow-cleaning, hand-washing, and recoating. This is especially true at LCOGT, and mirror maintenance is a mission-critical, but also costly operation in the worldwide distributed installation. To effectively balance the cost of CO<sub>2</sub> snow-cleaning, mirror washing, and recoating with the performance gain, LCOGT has started to closely monitor the throughput of all their telescopes. We presented the original concept and first data during the 2018 SPIE meeting,<sup>6</sup> and here we give an update with four more years of baseline data.

As outlined in,<sup>6</sup> the data-crawling phase of the monitoring application measures the throughput of the telescope by deriving the photometric zeropoint (and the color terms) of all science images obtained in the SDSS g’r’i’z’ filters by cross-referencing with the Atlas Refcat2 catalog.<sup>7</sup> This application is referred to as `photzp`. In the analysis stage, timelines of the photometric zeropoint for each of our telescopes are plotted. Fig. 4 for example compares the photometric zeropoint, i.e. the throughput, in the SDSS r’ band of the 2-meter telescopes at Haleakalā and Sutherland. These plots are updated daily and provide real-time feedback on the throughput of the telescopes.

As evident from the photometric zeropoint history plots, *individual* measurements are often not representative of the telescope throughput, for reasons such as non-photometric conditions, images being unintentionally out of focus, tracking errors, or mismatching of objects due to excessive crowding in the Galactic bulge. Yet, even with faulty measurements in the picture, the ensemble of data points remains extremely valuable as the upper envelope of all zeropoint measurements is a viable representation of a telescope’s throughput.

The `photzp` database now spans more than six years of throughput information of the LCOGT telescopes (with more than 1.3 million zeropoint measurements) and provides a unique insight into a telescope mirror cleaning strategy at the LCOGT sites.

#### 3.1.1 2-meter mirrors at Haleakalā and Siding Springs.

In Fig. 4 we show the photometric zeropoints in the SDSS r’ band for the two 2-meter telescopes in the LCOGT fleet, located on Haleakalā, Hawaii, and Siding Springs, Australia. The large upward steps in throughput reflect when the primary mirrors were recoated.

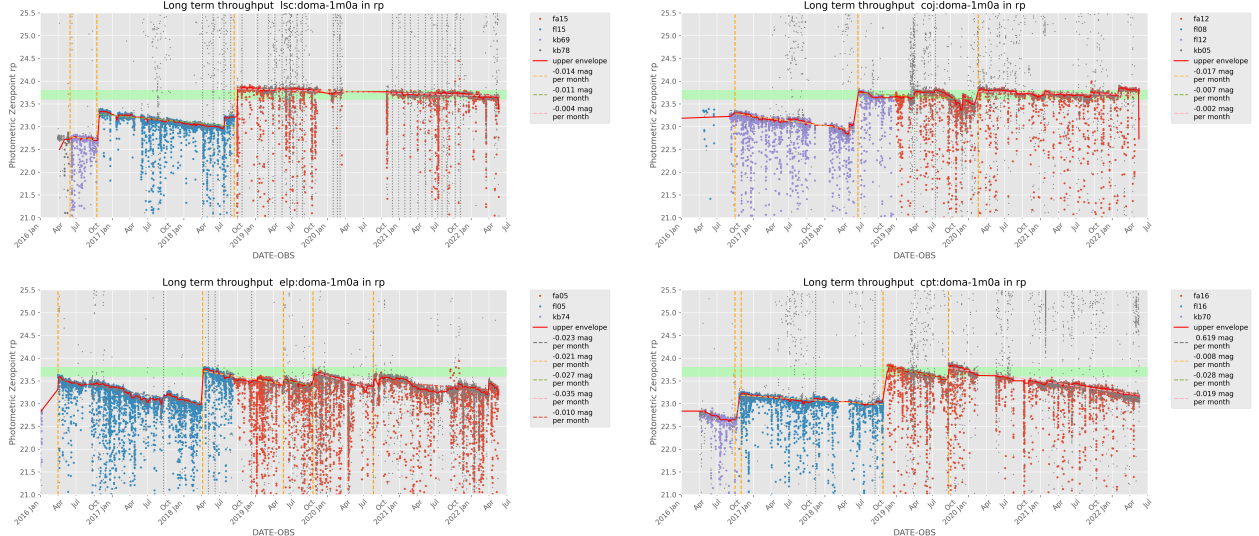


Figure 5. Comparison of the throughput of the LCOGT 1-meter telescopes in the SDSS  $r'$  band. From upper left to lower right: CTIO (Chile), Siding Springs (Australia), McDonald Observatory (Texas, USA), and Sutherland, South Africa.

While both two-meter telescope mirrors undergo similar regular CO<sub>2</sub> snow cleaning and washing, the faster degradation at the Siding Springs site is striking. As a consequence, we realuminized the mirror at this site in early 2021 and budget for more frequent recoatings.

### 3.1.2 1-meter mirrors at Cerro Tololo, Sutherland, Siding Springs, and McDonald Observatory

The comparison between the sites is particularly meaningful for the 1-meter telescope fleet as all those mirrors were recoated by the same vendor in 2018, and the initial conditions for mirror degradation are identical among those sites. We typically operate two to three 1-meter class telescopes at a site, and the throughput degradation of the mirrors at a site generally follows similar trends. In 2020, the operation of the 1-meter telescopes was interrupted due to COVID-19 in Chile, Texas, and South Africa, as evidenced by coverage gaps in Fig. 5. We notice:

- The CTIO site has the overall lowest throughput degradation rate (along with Haleakalā, but we lack a direct comparison with a 1-meter telescope there), consistent with a very low contamination rate (dust) of the mirrors and a very strict monthly CO<sub>2</sub> snow cleaning regimen. A similarly rigorous CO<sub>2</sub> snow cleaning schedule at the Siding Springs and Teide sites helps to maintain the throughput of the telescopes there as well.
- Unfortunately, we are not able to maintain a CO<sub>2</sub> snow cleaning schedule at the McDonald Observatory and Sutherland sites. However, at the McDonald site we found that a mirror wash can restore the throughput to a reasonable level. Due to travel restrictions, no LCOGT team could visit the Sutherland site for mirror washing during the last two years.
- In the summer of 2021 we installed two new 1-meter telescopes at the Teide site. The evidence of the positive impact of regular CO<sub>2</sub> snow-cleaning helped to convince the local site support of the importance of this task.

## 3.2 Case study: NRES acquisition unit's fiber pinhole location

The Network of Robotic Echelle Spectrographs (NRES,<sup>8,9</sup>) is LCOGT's most complex instrument. It is a network of four stabilized spectrographs with a resolution of  $R \sim 45000$  and a wavelength range from about 380 nm to 850 nm. Those spectrographs are located at the sites at Cerro Tololo (Chile), McDonald Observatory (Texas,

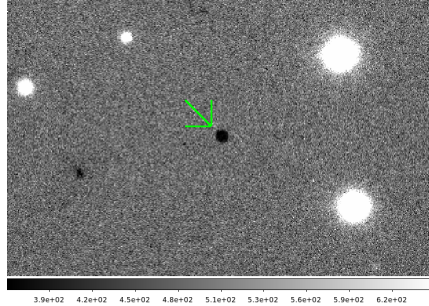


Figure 6. Zoom into the NRES science fiber pinhole region of the acquisition camera.

USA), SAAO (South Africa), and the Wise Observatory (Israel). Star light is fed into the spectrograph via an optical fiber at the telescope via the Acquisition and Guide unit (AGU). There, a mirror in the telescope's focal plane projects a guide image into a camera, and a pinhole in this mirror directs light into the fiber. An example image of the central pinhole is shown in Fig. 6.

The target acquisition is fully automated without human oversight.<sup>10</sup> The target acquisition software attempts to move the fiber pinhole under the target star, where the location of the pinhole as seen by the acquisition camera is configured in an instrument configuration file. The NRES AGU has no back-illuminator for the science fiber, and hence locating the fiber position is a manual, labor-intensive process based on the visual inspection of on-sky images.

Establishing the pinhole location was intended to be a one-time commissioning task, but after operating the first NRES unit in Chile for a while, it became evident that the location of the pinhole, as seen by the acquisition camera, is not entirely stable. The location of the pinhole is measured (centering a circle in `ds9` on the pinhole) and adjusted manually about once a month. To better understand how the pinhole was moving we started to automatically measure the pinhole location by cross-correlating the image around the pinhole with a circular template image. To avoid erroneous position measurements, we restrict images to:

1. Only autofocus sequence images, where no star should intentionally be located at or near the pinhole
2. Among those preselected images, ensure that the maximum flux level is similar to the background level of the image, i.e., there must be no accidental bright stars near the pinhole image.

Depending on the sky brightness and residual star contamination, each individual automated pinhole location measurement can still be (very!) wrong, but with a large number of data points, general trends are still discernible. Fig. 7 left shows examples of the measured AGU pinhole location, corrected for the mean location, over the operational time of the NRES spectrograph in Chile.

It became evident that there is a seasonal variation in the Y pixel location, whereas the X position of the pinhole remained very stable. Similar trends were subsequently found in all four NRES AGU units, to varying extents. The data set was further analyzed to demonstrate that flexure was not a cause for the moving pinhole, but there is a loose correlation with the ambient dome temperature. As the pinhole location plots are updated on a daily basis, we can now monitor in real-time when an update of the pinhole location lookup is warranted - until we find a better solution to reliably lock on the pinhole without human oversight, or ideally will be able to commit resources for a mechanical root cause analysis and redesign of the AGUs.

The large data set of the AGU pinhole locations established a baseline of *normal* behavior. Such a baseline is important to identify an error condition. An example is shown for the AGU unit at the NRES spectrograph in Israel, where we show in Fig. 7 (right) the history of the pinhole location for the spectrograph located at the Wise Observatory. Note that in this plot we unify the locations as seen by several different cameras, as cameras at the Wise site especially suffer from electronic failures - presumably due to exposure to corrosive dust.

We found early on that the pinhole location at this AGU was moving more rapidly, at first attributed to the more pronounced temperature swings at the site in Israel. A real problem became evident in August 2019 when

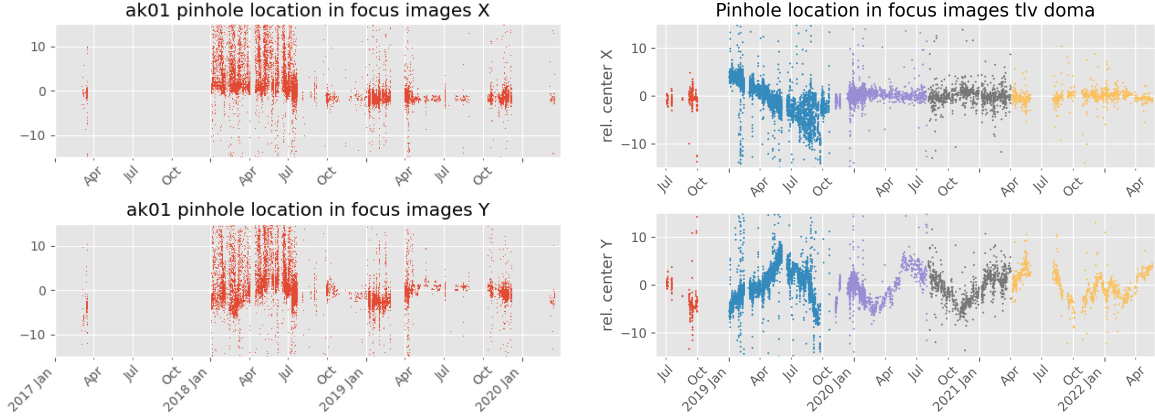


Figure 7. Time history of the pinhole location in the LSC dome B (CTIO) AGU, and the TLV dome A NRES AGU. The NRES acquisition unit in Chile has the longest history of operation, and it shows evidence of seasonal drifts in the pinhole location in the y-location, while the x location remains stable. The AGU at the Wise observatory (TLV) showed unusually strong seasonal drifts in the pinhole X location as well, with an unstable situation emerging in August 2019; this unusual behavior was traced to a loosened set screw in the camera mount.

the location of the X pinhole was starting to vary randomly. In fact, this issue prompted the creation of this monitoring application to both systematically understand the pinhole drift history and put it into context at other spectrographs. Thanks to those data we could identify the underlying problem as a mechanical problem with a clear directionality, and we could advise local site support staff of the rough area within the AGU where the problem might originate. In the end, a loose set screw that was (not) holding the acquisition camera in place was identified as the problem. Upon tightening that screw in Oct 2019, the pinhole location stabilized again. Unfortunately, this camera died shortly after and was subsequently replaced. The position swing along the Y-axis remains strong at the Wise Observatory site compared to other NRES installations. An athermal redesign of the acquisition and guide unit would be the ideal response to those findings.

### 3.3 Performance of the fleet of Archon CCD camera controllers

We have shown in 3.1 how the throughput of telescope and instrument optics are an important performance driver, but the performance of the detector system is of equal importance for an observatory’s efficiency. Every instrument’s manual or web page will feature a section that will highlight the read noise and conversion gain of the detectors. But when was this number revisited the last time? Usually, this number is established only once during commissioning and trusted ever after.

At LCOGT we are operating at least one science CCD camera per telescope, and for each telescope class, those cameras are of identical design. The imagers at the 2-meter and 1-meter telescopes revolve around Fairchild CCD486 detectors. The 2-meter telescopes use a commercial camera package and control electronics from Spectral Instruments, but the camera at Haleakalā has been replaced in 2020 with the MuSCAT3 instrument and uses Princeton Instruments Pixis and Sophia cameras. At the 1-meter telescopes, an in-house made cryostat system (Sinistro,<sup>1</sup>) is used. In 2018 we changed the CCD controllers of the Sinistro cameras to a STA Archon CCD<sup>§</sup> controller. The 40 cm telescopes use commercial SBIG 6303 cameras.

To monitor this plethora of imaging cameras we have created a crawler application that will measure the readnoise and gain of the cameras every day. We use the well-established method of measuring gain and readnoise from the shot noise and exposure level in pairs of flat fields and biases that we acquire daily as part of the LCOGT standard calibration plan.

Similar to the photzpz application, we use bias and sky flat fields that are already obtained daily as part of LCOGT’s calibration plan. Each day, sky flats from each camera are paired based on the filter and actual exposure level. We limit the noise and gain measurements to images taken in a subset of the available filters

<sup>§</sup>[www.sta-inc.net](http://www.sta-inc.net)

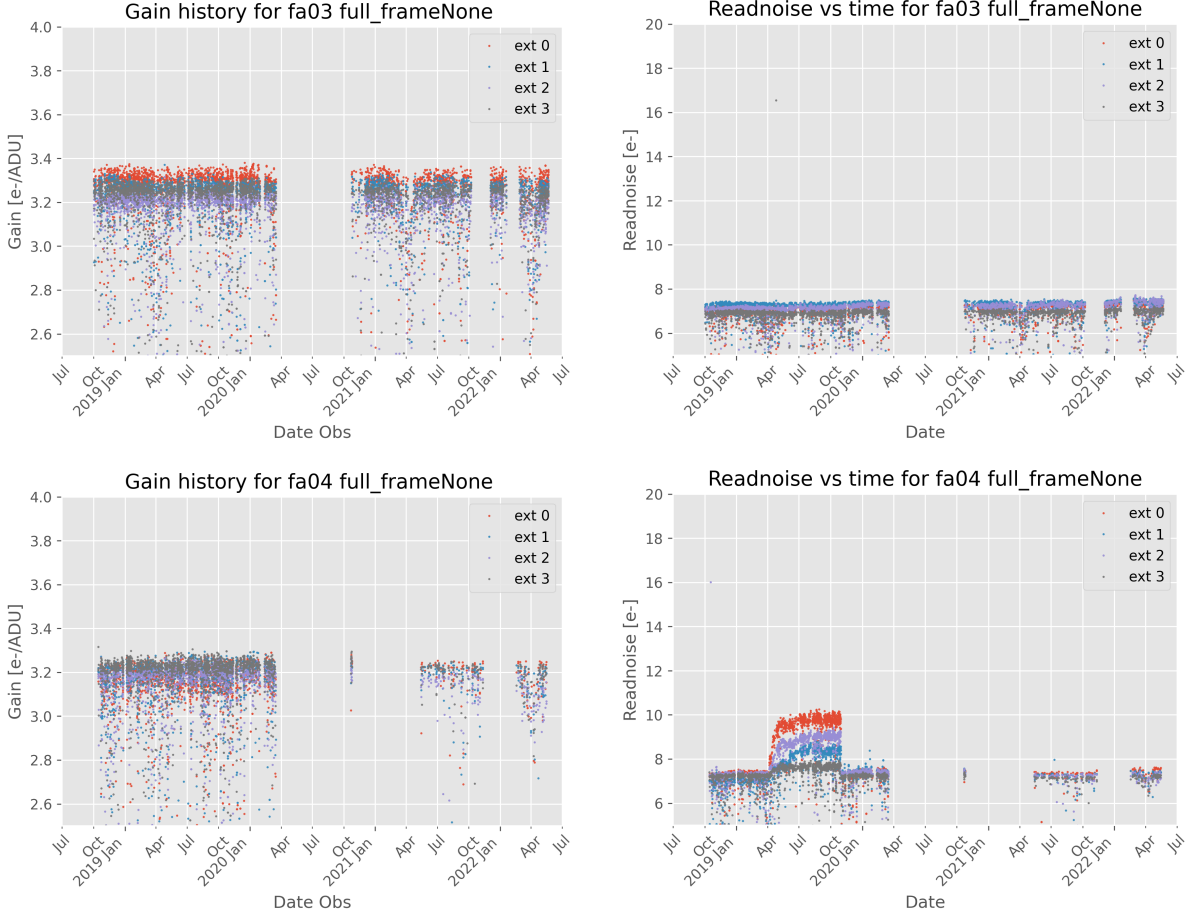


Figure 8. Timeline of readnoise and gain for two Sinistro CCD cameras operating with an Archon CCD controller. Each detector has four amplifiers, and data points are plotted per CCD amplifier (labeled as ext N, ext for extension). The camera fa04 (located in Chile) suddenly showed significant degradation in its noise behaviour (but note the constant gain), which traced to an issue in the A/D board in the controller.

to reduce systematic effects on the noise/gain measurement due to variation in the illumination level, e.g., due to fringing or large sensitivity variations in the near-UV bandpasses. Sometimes, flat fields images acquired in one twilight period in a filter might have varying exposure levels, despite the LCO site software attempting to compensate for the fading/brightening sky while taking flat field exposures in the morning and evening sky, and it is not unusual to not be able to automatically obtain a new measurement of the noise and gain.

We show examples of two Sinistro CCD cameras at the Cerro Tololo site in Fig. 8 where the Archon CCD controllers were installed at the same time. The noise and gain, for each of the four amplifiers, is shown. The camera fa03 shows steady operations over the entire life span, with only marginal seasonal variation in its readnoise, and a very steady gain.

The case of the camera fa04 however, shows how constant monitoring helped to identify the degradation of the CCD controller that started in April 2019, where the noise slowly increased from the typical 7-7.5 e- baseline to 10 e-. Note how the gain during this degradation was not changing at all. Since the camera controller was still operational, only with increased noise, this degradation in performance might have gone unnoticed in our automated data flow if not monitored.

Based on the findings from this performance monitoring, we asked on-site personnel in Chile to swap the controller between two telescopes, and we could establish that the increased noise was traveling with the CCD controller. Subsequently, it was decided to ship a replacement controller to Chile, and as of November 2019 the

noise performance of fa04 was restored.

The degradation of the Archon CCD controller showed a very distinct behavior for each of the four readout channels, and we have seen the same pattern occur at some Archon controllers at other sites as well. STA was able to trace the error to the A/D conversion board in the controller. We are still working closely with the vendor to replace the affected boards. Being able to provide consistent diagnostic tools for this failure mode was very helpful when communicating with the vendor to isolate the root cause, and to understand which production lot of A/D conversion boards were affected.

#### 4. CONCLUSION: THE CASE FOR ACCESSIBLE TELEMETRY DATA AND SCIENCE ARCHIVES TO SUPPORT OBSERVATORY OPERATIONS.

Traditional manual quality control and observatory oversight by observatory staff do not scale well to LCOGT's operational model of a large fleet of telescopes with the robotic operation and an automated data flow. We found that accessible telemetry plays a vital role in the day-to-day operation, but telemetry alone is not sufficient to understand the performance of the observatory. In response, we are now automatically executing typical commissioning tasks on science data taken every night and day from all telescopes. Presenting telemetry and performance data to staff requires careful design. With the addition of automated, telemetry-based alerts that are sent to appropriate first responders, we are further advancing the automation of our telescope network.

We gave examples of how LCOGT utilize easily accessible telemetry and science archive data to maintain situational awareness in our worldwide distributed network of telescopes. The combination of **OpenSearch** and **Grafana** allows various operational stakeholders such as mechanical engineers and the telescope operation group to create their data views and new alarms on existing telemetry without software programming knowledge, but expertise in the area of the monitored item. After an initial learning phase, this allowed for dynamic change in the alerting scheme by the interested parties with minimum support from the software and IT teams.

Installing, commissioning, and characterizing a new telescope or instrument is a daunting task by itself. By wrapping the tools created for the commissioning of a telescope or instrument in automated software frameworks, the commissioning tasks can become part of an effective operations and quality assurance model.

#### REFERENCES

- [1] Brown, T. M., Baliber, N., Bianco, F. B., Bowman, M., Burleson, B., Conway, P., Crellin, M., Depagne, É., De Vera, J., and Dilday, B., "Las Cumbres Observatory Global Telescope Network," *PASP* **125**, 1031 (Sep 2013).
- [2] Saunders, E. S., Lampoudi, S., Lister, T. A., Norbury, M., and Walker, Z., "Novel scheduling approaches in the era of multi-telescope networks," in [*Observatory Operations: Strategies, Processes, and Systems V*], *Society of Photo-Optical Instrumentation Engineers (SPIE) Conference Series* **9149**, 91490E (Aug 2014).
- [3] Volgenau, N., Bowman, M., Conway, P., Haworth, B., Heinrich-Josties, E., Kirby, A., Rettinger, S., and Riba, A., "Las Cumbres Observatory's end-to-end operations workflow," in [*Observatory Operations: Strategies, Processes, and Systems VIII*], *Society of Photo-Optical Instrumentation Engineers (SPIE) Conference Series* **11449**, 1144907 (Dec. 2020).
- [4] McCully, C., Turner, M., Volgenau, N., Harbeck, D., Valenti, S., Riba, A., Bachelet, E., Snyder, I. W., Kurczynski, B., and Norbury, M., "Lcogt/Banzai: Initial Release," (Jan 2018).
- [5] McCully, C., Volgenau, N. H., Harbeck, D.-R., Lister, T. A., Saunders, E. S., Turner, M. L., Siiverd, R. J., and Bowman, M., "Real-time processing of the imaging data from the network of Las Cumbres Observatory Telescopes using BANZAI," in [*Software and Cyberinfrastructure for Astronomy V*], *Society of Photo-Optical Instrumentation Engineers (SPIE) Conference Series* **10707**, 107070K (Jul 2018).
- [6] Harbeck, D.-R., McCully, C., Pickles, A., Volgenau, N., Conway, P., and Taylor, B., "Long-term monitoring of the throughput in Las Cumbres Observatory's fleet of telescopes," in [*Proc. SPIE*], *Society of Photo-Optical Instrumentation Engineers (SPIE) Conference Series* **10704**, 1070401 (July 2018).
- [7] Tonry, J. L., Denneau, L., Flewelling, H., Heinze, A. N., Onken, C. A., Smartt, S. J., Stalder, B., Weiland, H. J., and Wolf, C., "The ATLAS All-Sky Stellar Reference Catalog," *ApJ* **867**, 105 (Nov. 2018).

- [8] Eastman, J. D., Brown, T. M., Hygelund, J., van Eyken, J., Tufts, J. R., and Barnes, S., [*NRES: the network of robotic Echelle spectrographs*], vol. 9147 of *Society of Photo-Optical Instrumentation Engineers (SPIE) Conference Series*, 914716 (2014).
- [9] Siverd, R. J., Brown, T. M., Barnes, S., Bowman, M. K., De Vera, J., Foale, S., Harbeck, D.-R., Henderson, T., Hygelund, J., and Kirby, A., “NRES: the network of robotic echelle spectrographs,” in [*Ground-based and Airborne Instrumentation for Astronomy VII*], *Society of Photo-Optical Instrumentation Engineers (SPIE) Conference Series* **10702**, 107026C (Jul 2018).
- [10] Foale, S., Bowman, M. K., Nation, J. S., Harbeck, D. R., and Siverd, R. J., “Robotic acquisition of spectrograph targets across the Las Cumbres Observatory global network of telescopes,” in [*Proc. SPIE*], *Society of Photo-Optical Instrumentation Engineers (SPIE) Conference Series* **10707**, 107070Y (July 2018).